Mon. Not. R. Astron. Soc. **000**, 1–11 (2004) Printed 2 February 2008 (MN LATEX style file v2.2)

Optical line profiles of the Helix planetary nebula (NGC 7293) to large radii.

J. Meaburn[1], J. A. López [2] and M. G. Richer[2].

[1] *Jodrell Bank Observatory, Dept of Physics & Astronomy, University of Manchester, Macclesfield, Cheshire SK11 9DL UK.*

[2] *Instituto de Astronomía, UNAM, Apdo. Postal 877, Ensenada, B.C. 22800, México.*

Accepted yyyy mmmmmmmmmm dd. Received yyyy mmmmmmmmmm dd; in original form yyyy mmmmmmmmmm dd

ABSTRACT

New, very long (25′), cuts of spatially resolved profiles of the Hα and [N II] optical emission lines have been obtained over the face of the Helix planetary nebula, NGC 7293. These directions were chosen to supplement previous similar, though shorter, cuts as well as crossing interesting phenomena in this nebular envelope. In particular, one new cut crosses the extremes of the proposed CO J=2-1 emitting outer 'torus' shown by Huggins and his co–workers to be nearly orthogonal to its inner counterpart. The second new cut crosses the extensive outer filamentary arcs on either side of the bright nebular core. It is shown that NGC 7293 is composed of multiple bipolar outflows along different axes. Hubble-type outflows over a dynamical timescale of 11,000 yr are shown to be occurring for all of the phenomena from the smallest HeII emitting core out to the largest outer filamentary structure. All must then have been ejected over a short timescale but with a range of ejection velocities.

Key words: circumstellar matter: Helix Nebula: NGC 7293

1 INTRODUCTION

The Helix planetary nebula (NGC 7293) continues to attract both observational and theoretical interest simply because it is one of the closest (213 pc distant – Harris et al. 1997) bright, evolved planetary nebulae (PNe) and hence open to investigation on a wide range of spatial scales. In both O'Dell, McCullough & Meixner (2004) and Meaburn et al. (2005b), and references therein, much of the previous work is summarised up to those dates. More recently, Hora et al. (2006) have made Spitzer Space Telescope infra-red observations where the knotty nature of the whole PN envelope is spectacularly apparent in their images. Ultra-violet (UV) images of NGC 7293 released in 2005

and taken with the Galaxy Evolution Explorer (GALEX) satellite reveal particularly well many of the halo features including what was thought to be the large filamentary bipolar lobe as well as a possible 'jet' and the counter bow-shaped feature previously noted in [N II] 6584 Å emission by Meaburn et al. (2005b). (The GALEX FUV (135-175 nm) image combined with the NUV (175-280 nm) one can be examined in photojournal.jpl.nasa.gov/jpeg/PLA07902.jpg). Theoretically, Dyson et al (2006) have predicted the creation of the unambiguously accelerating tails of the inner toroidal system of cometary knots as their dense core are overrun by the mildly supersonic AGB 'superwind'. Garcia-Segura et al (2006) have also considered the effects on the PN envelope as the highly supersonic 'fast' wind switched off for this is no longer observed in the spectrum of the central star (Cerruti–Sola & Perinotto 1985).

The global structure of the complex PN envelope of NGC 7293 is becoming clarified for the key to its understanding is knowledge of its large–scale kinematical behaviour. Initially, Meaburn & White (1982) from wide-field Fabry-Perot line profiles and imagery using the [N II] 6584 Å and [O III] 5007 Å emission lines showed that the helical appearance of the bright core of NGC 7293 is the manifestation of a bipolar shell expanding at ≈ 25 km s^{-1} viewed at a 37° to its axis. This central bipolar structure was also shown to contain an inner [O III] 5007 Å emitting spherical shell now (Meaburn et al 2005b) known to be expanding at only 12 km s^{-1}. Healey & Huggins (1990) and Young et al (1999) with complete coverage of CO J=2–1 profiles over the bright, apparently helical structure refined this viewpoint and furthermore suggested that the bipolar lobes emanated from a central, clearly identifiable, torus expanding at 29 km s^{-1}. Incidentally, this central structure, with two diametrically opposite, elongated, expanding shells emanating from a central expanding torus will be referred to throughout this paper as 'bipolar' in keeping with its previous description (see fig.11 in Meaburn et al. 2005). Overall it could equally be described as a quasi-ellipsoidal expanding structure with a dense, toroidal waist. All features of this model for the bright helical structure were consolidated by the morphological/kinematical modelling of the optical observations in Meaburn et al. (1998 & 2005b). The spatially resolved [N II] 6584 Å profiles with the first Manchester Echelle Spectrometer (MES – Meaburn et al 1984) on the Anglo-Australian 3.9–m telescope over 17′ diameter east–west and north–south cuts (6 & 7 in Fig. 1) (Meaburn et al 1996 & 1998) proved decisive in this analysis.

These previous long cuts of optical line profiles have now been supplemented by even longer cuts at intermediate and strategically desirable position angles over the nebular surface. Of particular interest are the anomalous velocity features in the CO J=2–1 profiles discovered by Healey & Huggins (1990) and mapped completely by Young et al (1999) which suggests that there is a

separate neutral torus, not seen hitherto in the imagery or line profiles at optical wavelengths but which is both outside the nebular core and expanding nearly orthogonally to it. One of the new extra-long cuts of optical line profiles, to be reported here, crosses both the 'point symmetric' CO features (see fig. 3 of Young et al 1999) that lead to this orthogonal interpretation, as well as being orientated nearly down the axis of the proposed 'inner' bipolar lobe. The second new extra-long cut crosses the main 'helical' structure but extends continuously out to the faint halo filaments on either side of this and along the inner part of a possible jet. Only limited observations of the optical line profiles from the north-eastern halo filaments had been made previously (Walsh & Meaburn 1987; Meaburn et al 2005b though note the calibration correction made for the latter in the present paper).

The combination of these new observations with the previous long cuts of optical line profiles now provides unprecedented kinematical coverage of the principal features of NGC 7293. Consequently, the propensity in PNe for the ejection of multiple bipolar lobes, each perpendicular to its own expanding torus themselves at various tilt angles, is clearly revealed in NGC 7293.

2 OBSERVATIONS AND RESULTS

The longslit observations were obtained with the Manchester Echelle Spectrometer (MES–SPM Meaburn et al, 2003) combined with the f/7.9 focus of the 2.1–m San Pedro Mártir UNAM telescope between 29 July and the 29 Aug. 2005. This echelle spectrometer has no cross-dispersion. For the present observations, a filter of 90 Å bandwidth was used to isolate the 87^{th} order containing the Hα and [N II] nebular emission lines.

A SITE CCD with 1024 $\times$ 1024 square pixels, each with 24 μm sides, was the detector. Two times binning was employed in both the spatial and spectral dimensions. Consequently 512 increments, each 0.624$''$ long, gave a total projected slit length of 5.32$'$ on the sky. 'Seeing' varied between 1-2$''$ during these observations.

Six overlapping slit positions were obtained along each of the two cuts 4 and 5 in Fig. 1. These were each merged to form the single positional– velocity (pv) arrays of Hα and [N II] 6584 Å profiles using the Starlink KAPPA CCDPACK MAKEMOS routines. Only the [N II] 6584 Å arrays after this process are shown in Figs 2 & 3 for PA = 76° and 140° respectively for the Hα profiles are emitted by the whole of the internal expanding volumes of NGC 7293 (Meaburn et al 2005b) and the final picture becomes confused.

The slit was 150 μm wide ($\equiv$ 11 km s^{-1} and 1.9$''$) for ten of the separate slit positions and

300 μm wide for only the two positions at either end of cut 5. Integration times were 1800 s in all cases and the spectra were calibrated in wavelength to $\pm$ 1 km s^{-1} accuracy when converted to heliocentric radial velocity ($V_{\rm hel}$) against the spectrum of a Th/Ar arc lamp.

Incidentally, there is an error in the velocity scale of figs 3–5 in Meaburn et al (2005b) for the pv arrays from slit positions 1-3 (shown here in Fig. 1). The heliocentric correction had not been applied to the velocity scale, consequently the zero of the erroneous scales in these previous figures should be -26.1 km s^{-1} to convert them to heliocentric radial velocity. This has been carried out for the pv array of [N II] 6584 Å profiles for slit position 2 in Fig. 1 and shown here in Fig. 5. The [N II] 6584 Å profiles are compared in Fig. 5 with the systemic heliocentric radial velocity $V_{\rm sys}$ = -27 $\pm$ 2 km s^{-1} for the whole nebula (Meaburn et al 2005b - and see therein details of these previous observations). Note that for comparison with the CO observations of Young et al (1999) their relationship $V_{\rm hel} = V_{\rm lsr}$ - 3.2 km s^{-1} should be used though the STARLINK RV routine gives the difference as either -1.9 or -2.9 km s^{-1}.

3 DISCUSSION

3.1 The morphology of the large–scale features.

Many of the large–scale optical phenomena are sketched in Fig. 6 as dark solid lines for the brighter features and dark dashed lines for the fainter ones. These can be seen in the deep Hα + [N II] 6548, 6584 Å image presented in fig. 1a-c of Meaburn et al (2005b) and spectacularly in the near UV (175–280 nm) Galaxy Evolution Explorer (GALEX) image (NASA/JPL–Caltech/SSC circulated in 2005). The faint nebulosity visible in the latter image may be a consequence of the dominant C III] 1906 & 1909 Å emission lines. The bright [N II] 6584 Å emitting central inner 'ring' in Fig. 6 is on the inside edge of a corresponding CO J=2-1 emitting ring (Huggins & Healy 1986; Healy & Huggins 1990 and Young et al 1999) expanding at 29 km s^{-1} yet surrounds the system of slower moving cometary knots whose expansion is only 14.5 km s^{-1} (Meaburn et al 1996). Bipolar lobes project (Meaburn et al 1996& 2005b) along the common axis of these ionized/neutral tori. The lobes of this central bipolar system manifest themselves as the bright helical filaments in Fig. 6.

Young et al (1999) reveal clearly the presence of an outer CO expanding ring whose curve of radial velocities (their fig. 5) shows that it is orientated nearly orthogonally to its inner companion. The sides of this outer ring with its highest approaching and receding radial velocities are depicted in Fig. 6 by the southeastern and northwestern hashed 'CO' circles respectively. It is notable that

the axis of this outer CO torus has approximately the same position angle (PA = 140°) as the faint extensions marked L1 and L2 in Fig. 6.

The jet–like feature and its possible bow–shaped filamentary counterpart are also very clear in the UV GALEX image. The possible jet extends from inside the image of the filaments of the SW outer arc to the edge of the outer envelope and because of the tentative identification of its nature is marked jet? in Fig. 6.

3.2 The kinematics of the large–scale features

3.2.1 Inner bipolar structure along PA = 125°.

The detailed kinematical–morphological modelling in Meaburn et al (2005b) of the pv arrays of [N II] 6584 Å profiles along the previous cuts 6 & 7 in Fig.1 showed that the bright helical filaments and inner ring in Fig. 6 are the manifestations of an inner bipolar nebula with a central expanding torus. In this model the axis of the central torus is taken to be along PA $\approx$ 125°, orientated at 37° to the sight line and expanding at 14.5 km s^{-1} i.e. the expansion velocity of the system of cometary knots. The lobes are expanding with Hubble–type velocities and reach expansion velocities of 24 km s^{-1}. The southeastern and northwestern lobes are tilted towards and away from the observer respectively. The tilt of the bipolar axis and that of the central torus with respect to the sight line was determined simply by measuring the apparent dimensions of the ring (see Fig. 6) in optical images and by assuming the torus is circular.

This interpretation is consolidated in detail by the new profiles over this core along cuts 4 & 5 in Figs. 2 & 3 respectively. The line profiles of the inner [N II] 6584 Å emitting ring of the central torus is revealed particularly well in Fig. 2, along cut 4, which is aligned nearly with the bipolar axis at PA = 125°. Here its emission manifests itself as the two brightness maxima at 4′ and -4′ from the central star at radial velocities of $V_{\rm hel}$ = -36.7 $\pm$ 1 and -11.2 $\pm$ 1 km s^{-1} respectively. These measurements were made by Gaussian fitting the single line profiles extracted from those parts of the pv arrays containing the maxima. The expansion velocity of the [N II] 6584 Å emitting torus can now be refined compared with the 14.5 km s^{-1} (the expansion velocity of the system of cometary knots) used in the model in Meaburn et al (2005b). With this direct measurement this becomes 12.75 (sin 37°)$^{-1}$ = 21.2 km s^{-1}. A systematic change in expansion velocity throughout the inner neutral/ionized torus is then occurring with the system of cometary knots nearest the central star expanding at 14.5 km s^{-1}, the larger diameter intermediate [N II] 6584 Å part of the

torus (the 'ring' in Fig. 6) at 21.2 km s^{-1} and the outermost CO component of this central torus (Young et al 1999) at 29 km s^{-1}.

The change of expansion velocity of the central [N II] 6584 Å emitting torus from 14.5 to 21.2 km s^{-1} in the morphological/kinematical model in Meaburn et al (2005b) makes only minor cosmetic differences to the predictions of the model for comparison with the previous observations along cuts 6 & 7 in Fig. 1. In fact, the detailed comparison is improved quantitatively but will not be repeated here. The tilt to more positive velocities from the southeastern to the northwestern (bottom to top) is clear in Fig. 2 as predicted by the same bipolar/torus model.

3.2.2 Outer CO torus

Firstly, the outer CO ring appears to have been detected at optical wavelengths for the first time in the new pv array along cut 4. The very deep, negative, greyscale image of this is presented in Fig. 4 and two sets of velocity 'spikes' (A and B in Fig. 4) can be seen over the approaching and receding maxima depicted in Fig. 6. These have the same radial velocity ranges as the corresponding CO features of Young et al (1999). The higher angular resolution of the present [N II] 6584 Å data compared with the CO maps (30″) appears to have resolved this outer neutral/ionized torus into a double ring structure with its axis along PA = 140° compared with PA = 125° for the inner torus (Sect. 3.2.1). There is no easy way to estimate directly the tilt of the axis of this outer torus to the sight line for it does not appear on optical images and most of its extent gets confused in the CO maps as it crosses the central nebula, consequently an estimation of only a lower limit of its expansion velocity can be made i.e. $\geq$ 27 km s^{-1}. The possible bipolar lobes L1 and L2 in Fig. 6 (Sect. 3.1.1) associated with this outer torus would have receding and approaching radial velocities respectively. Neither have yet been measured. Also the axis of the outer CO torus and the common axis of these possibily related bipolar lobes would expected to be the same.

3.2.3 Outer bipolar structure along PA = 50°.

Evidence for some type of outer bipolar structure, as suggested on morphological grounds in Sect. 3.1, enveloping the inner one, is also present in this new kinematical data. As the pv array crosses from the bright helical structure to the NE outer arc in Fig. 3 along cut 5 the profiles stay on $V_{\rm hel}$ = -50 km s^{-1}until they reach -95 km s^{-1} to then come back to $V_{\rm sys}$ = -27 km s^{-1} at the bright filamentary edge. Similar behaviour is shown in Fig. 5 for the previous pv array along slit 2. Some sort of three dimensional expansion at $\geq$ 68 km s^{-1} must be occurring with the bright NE outer

arc filaments being viewed tangentially through the edge of an expanding shell. However, this partial (?) shell cannot have a simple, radially expanding, quasi-spherical structure for no receding velocities are detected within its circumference.

The pv arrays in Fig. 3 for the southwestern end of cut 5 cover the filamentary feature that could be an inner extension of the 'jet' in Fig. 6. Within this complication, radial velocities are in receding directions as the SW outer arc is crossed which is consistent with the NE and SW outer arcs in Fig. 6 being part of the same, albeit not simple, bipolar structure.

3.2.4 Jet and bow–shock

Only very limited information is in the present kinematical data concerning the nature of the possible jet and bow–shock whose morphology is discussed in Sect. 3.1. The most telling behaviour is the Hubble–type increase in radial velocity along the possible inner part of the jet as shown along the southwestern end of the pv array in Fig. 3. The radial velocities in the knots in the 'jet' change systematically from $V_{\rm hel}$ = -10 km s^{-1} at about -8′ from the central star out to $V_{\rm hel}$ = 10 km s^{-1} at the bottom end of the array. Unfortunately the jet-like feature nearest the outer envelope was not covered in the present observations.

No direct kinematical information has yet been obtained over the bow–shaped filament in the northwestern quadrant (Fig. 6). However, the UV GALEX image reveals this to be the edge of extensive complex filamentary structure up to the central bright helical filaments and the outer arc may only be the edge of a three dimensional structure typical of bow-shocks. In this case it could be possible that the extreme velocity feature out to $V_{\rm hel}$ = -110 km s^{-1} at 6′ from the central star along cut 5 in Fig. 3 is from this more extended structure. More observations are needed to investigate this possibility conclusively.

4 EPISODIC EJECTIONS WITHIN A HUBBLE-TYPE OUTFLOW.

Further evidence is presented here that NGC 7293 is composed of at least two bipolar nebulae, with their bipolar axes at substantially different orientations along PAs = 125° and 50° respectively. The tilt of the axis of the the PA = 125° lobes are well- established as 37° with respect to the sight line whereas that of the PA = 50° lobes is as yet unknown. This multiple bipolar lobe structure is common in other 'poly-polar' nebulae e.g. NGC 6302 (Meaburn & Walsh 1980), KjPn 8 (López, Vazquez & Rodriguez 1995: López et al 1997), NGC 2440 (López et al 1998), J 320 (Harman et al 2004) and see Manchado et al (1996). In fact this multi-polar structure represents the rule in young

Table 1. The expansion velocities for distinct components of NGC 7293 are listed versus their radii.

EXPANSIONS v. RADII

feature	**radius**	**expansion velocity**	**references**
1) HeII central volume	$\leq 1.6'$	≤ 12 km s^{-1}	O'Dell et al 2004: Meaburn et al 2005b
2) [OIII] inner shell	$2.2'$	12.5 km s^{-1}	Meaburn & White 1982: Meaburn et al 2005b
3) cometary globules	$3.0'$	14.5 km s^{-1}	Meaburn et al 1992
4) inner torus - [NII]	$4.0'$	21.2 km s^{-1}	present paper
5) inner torus - CO	$4.3'$	29.0 km s^{-1}	Young et al 1999
6) inner torus - [NII] lobes	$5'$	24 km s^{-1}	Meaburn et al 2005b
7) outer torus - CO	$\geq 3.8'$	≥ 27 km s^{-1}	Young et al 1999
8) NE outer arc	$\approx 12.5'$	≥ 68 km s^{-1}	present paper

proto–PNe (Su et al. 2003) and the evolved PN NGC 7293 is most likely the natural descendent of this early structure.

The radii and expansion velocities of the proposed bipolar outflows for NGC 7293 are summarised in Table 1 and plotted in Fig. 7. Also included are the radii and expansion velocities of the inner HeII 4686Å & 6560Å emitting volumes, the inner [O III] emitting shell and the system of cometary globules. The most striking feature of the trends in Fig. 7 is that Hubble–type expansion is occurring continuously from the innermost volumes of NGC 7293 right out to the NE outer arc (8 in Fig. 7). The simplest dynamical interpretation of such behaviour is that all features must have been formed over a short period of time compared with the dynamical age of the nebula, in a sequence of ejection events, sometimes along different axes; the fastest ejections in a particular direction could have simply travelled furthest and, if knotty (Hora et al. (2006), separated out from those moving slower. This Hubble–type expansion is not unexpected for it has been found in many younger PNe (Corradi 2004). .

Most recently, from observations of the UV absorption line profiles in the spectrum of the hot central star of the Dumbbell nebula (NGC 6853, M27) McCandliss et al (2007) and McCandliss & Kruk (2007) have consolidated in detail the same viewpoint (also see Meaburn et al 2005a) for this similarly evolved PN. Wilson (1950) had come to the same conclusion for many bright PNe.

The present observations of the [N II] radius and expansion velocity (see 4 in Table 1) of the inner torus of NGC 7293 then offer a sound estimation of the dynamical age T_D = 11,000 yr of the whole nebula for a distance of 213 pc (Sect. 1) and within the Hubble - type expansion assumption. This is consistent with the estimation of T_D = 10,000 yr for the inner CO emitting torus by Young et al (1999).

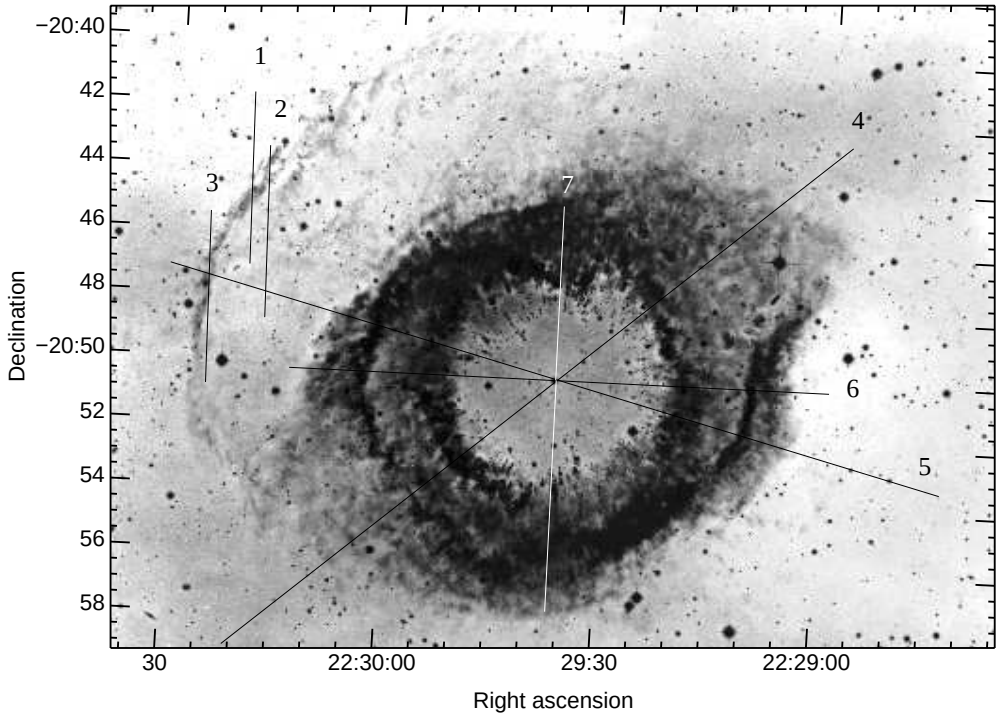

Figure 1. The previous slit positions and long cuts of spatially resolved profiles 1, 2, 3, 6 and 7 and new ones, 4 and 5 are shown against the unsharp masked R image of NGC 7293 taken at the f/3.3 prime focus of the Anglo–Australian telescope by Malin (1982). The coordinates are 2000 epoch.

ACKNOWLEDGEMENTS

JM is grateful to UNAM for supporting his 2007 visit to the Instituto de Astronomía, Ensenada where this paper was initiated and to Myfanwy Lloyd (né Bryce) for advice on the use of the MAKEMOS Starlink routines. JAL and MGR are in grateful receipt of DGAPA - UNAM grants IN 112103, 108406-2 and 108506.

REFERENCES

Corradi, R. L. M., 2004, Asymmetrical Planetary Nebulae III, M. Meixner, J. H. Kastner, B. Balick and N. Soker eds., AsP Conf. Ser. Vol. 313, p148.

Cerruti–Sola, M.& Perinotto, M. 1985, ApJ, 291, 237.

Dyson J. E., Pittard J. M., Meaburn J. & Falle S. A. E. G., 2006, A&A, 457, 561.

Garcia-Segura G., López J. A., Steffen W., Meaburn J. & Manchado A., 2006, ApJL, 646, 61.

Harman, D. J., Bryce, M., López, J. A., Meaburn, J. & Holloway, A. J. 2004, MNRAS, 348, 1047.

Harris, H. C., Dahn, C. C., Monet, D. G. & Pier, J. R. 1997, in IAU Symposium 180, eds. H. J. Habing & H. J. G. J. M. Lambers (Dordrecht: Reidel), 40.

Healey A. P.& Huggins P. J. 1990, AJ, 100, 511.

Hora J. L., Latter W. B., Smith H. A. & Marengo, M., 2006, ApJ, 652, 426.

Huggins P. J. & Healey A.P., 1986, ApJL, 305, 29.

López, J. A., Vazquez R. & Rodriguez L. F., 1995, ApJ, 455, 63.

López, J. A., Meaburn, J., Bryce, M. & Rodriguez, L. F., 1997, ApJ, 475, 705.

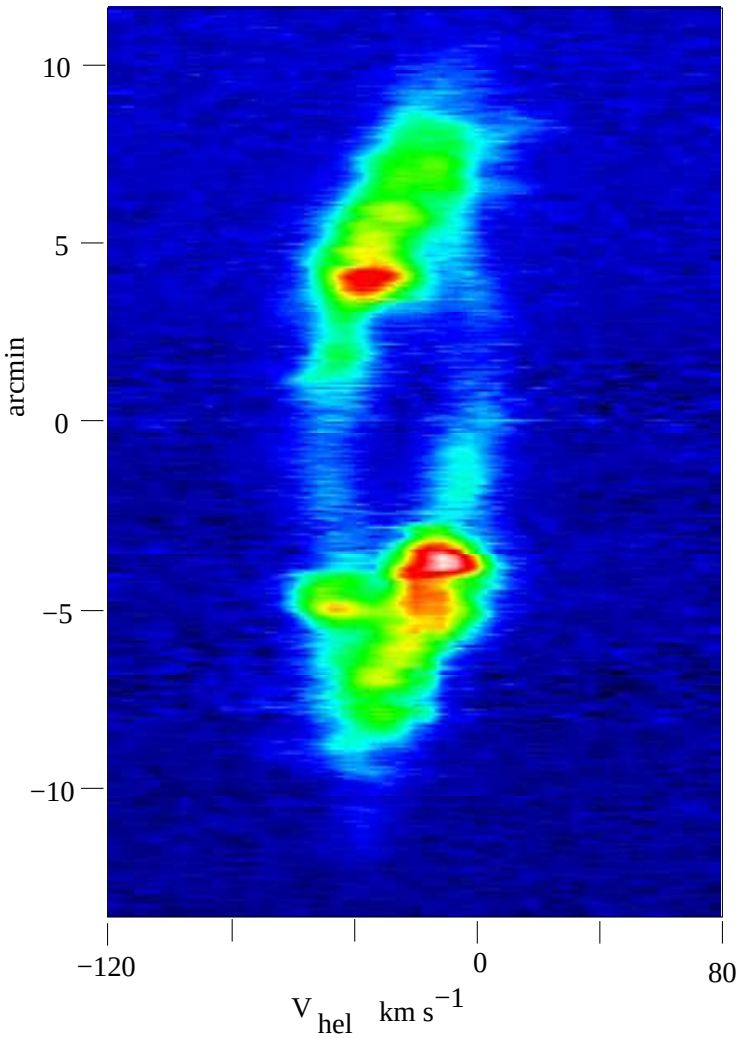

Figure 2. A positional–velocity display of [N II] 6584 Å line profiles along the new cut number 4 in Fig. 1 is shown. The vertical axis is the offset from the central star (the horizontal continuous spectrum) and the south eastern quadrant is to the bottom. This array is composed of the merged spectra from six separate but overlapping slit positions. The surface brightnesses have been converted to their natural logarithmic values and the colours used in the display are equally separated on this natural logarithmic scale.

López, J. A., Meaburn, J., Bryce, M. & Holloway, A. J., 1998, ApJ, 493, 80.

Malin, D. F., 1982, Sky and Telescope, 63, 22.

Manchado, A., Stanghellini, L. & Guerro, M. A., 1996, ApJ, 466, 95.

McCandliss, S. R., France, K., Lupu, R., Burgh, B. B., Sembach, K., Kruk, J., Andersson, B.-G. & Feldman, P. D., 2007, ApJ, 659, 1291.

McCandliss, S. R. & Kruk, J., 2007, ApJS, 170, 126.

Meaburn, J. & Walsh, J. A. 1980, MNRAS, 193, 631,

Meaburn J., Blundell B., Carling R., Gregory D. F., Keir D. & Wynne C., 1984, MNRAS, 210, 463.

Meaburn J., Clayton C. A., Bryce M. & Walsh J. R. 1996, MNRAS, 281, L57.

Meaburn J., Clayton C. A., Bryce M., Walsh J. R., Holloway A. J. & Steffen W. 1998, MNRAS, 294, 201.

Meaburn J. & White N. J., 1982, Astrophys. Space Sci., 82, 423.

Meaburn, J., López, J. A., Gutiérrez, L., Quiróz, F., Murillo, J. M., Valdéz, J. & Pedrayez, M., 2003, RevMexAA, 39, 185.

Meaburn J., Boumis P., Christopoulou P. E., Goudis, C. D., Bryce M. & López, J. A., 2005a, Rev. Mex. AA, 41, 109.

Meaburn J., Boumis P., López, J. A., Harman, D. J. Bryce M., Redman M. P. & Mavromatakis F., 2005b, MNRAS, 360, 963.

O'Dell C. R., McCullough P. & Meixner M., 2004, AJ, 128, 2339.

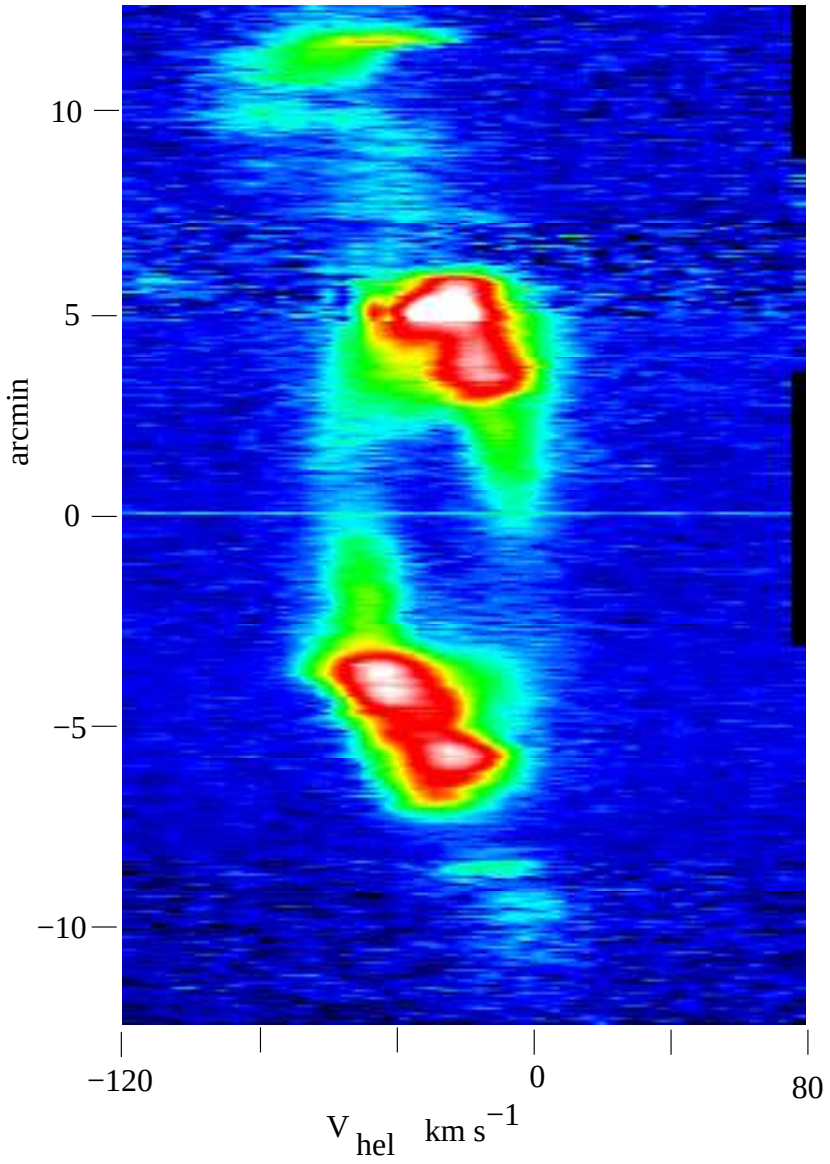

Figure 3. As for Fig. 2 but for cut 5 in Fig. 1. The south–western quadrant is to the bottom.

Su, K. Y. L., Hrivnak, B. J., Kwock, S. & Sahai, R., 2003, AJ, 126, 8485.

Walsh, J. R. & Meaburn, J., 1987, MNRAS, 224, 885.

Wilson, O. C., 1950, ApJ, 111, 279.

Young, K., Cox, P., Huggins, P. J., Forveille, T. & Bachiller, R., 1999, ApJ, 522, 387.

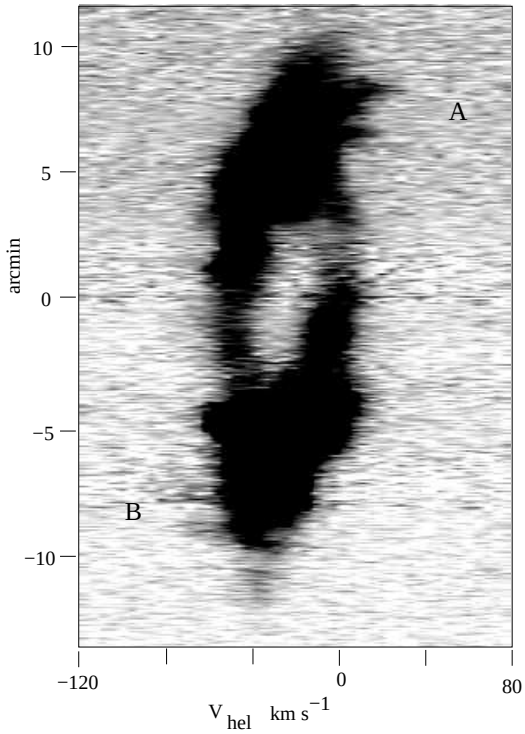

Figure 4. A very deep, negative, greyscale representation of the same positional velocity array as shown in Fig. 2. The velocity 'spikes' marked A and B match in position and extent the comparable CO features. The faint [N II] 6584 Å profiles across the south–eastern halo can also be seen at the bottom of the display.

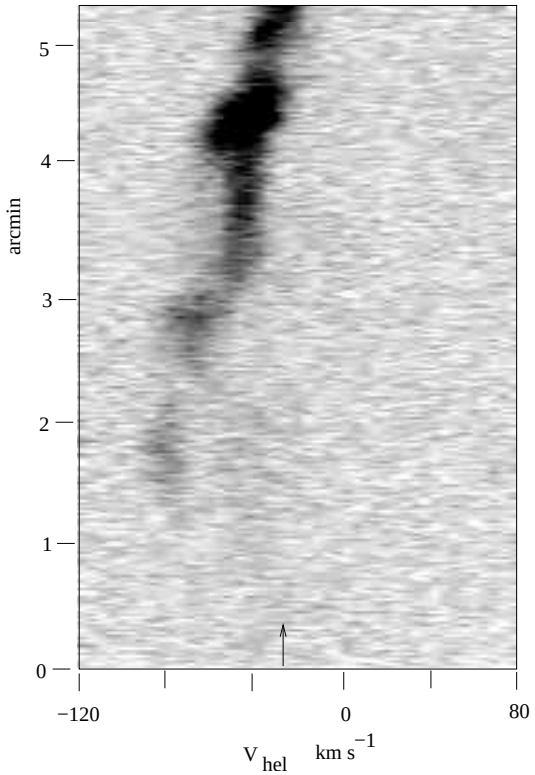

Figure 5. The positional-velocity array of [N II] 6584 Å profiles from the previous slit position 2 in Fig. 1 is presented now with the corrected $V_{\rm hel}$ (see text). This array is compared with the systemic heliocentric radial velocity (arrowed) of the whole nebula.

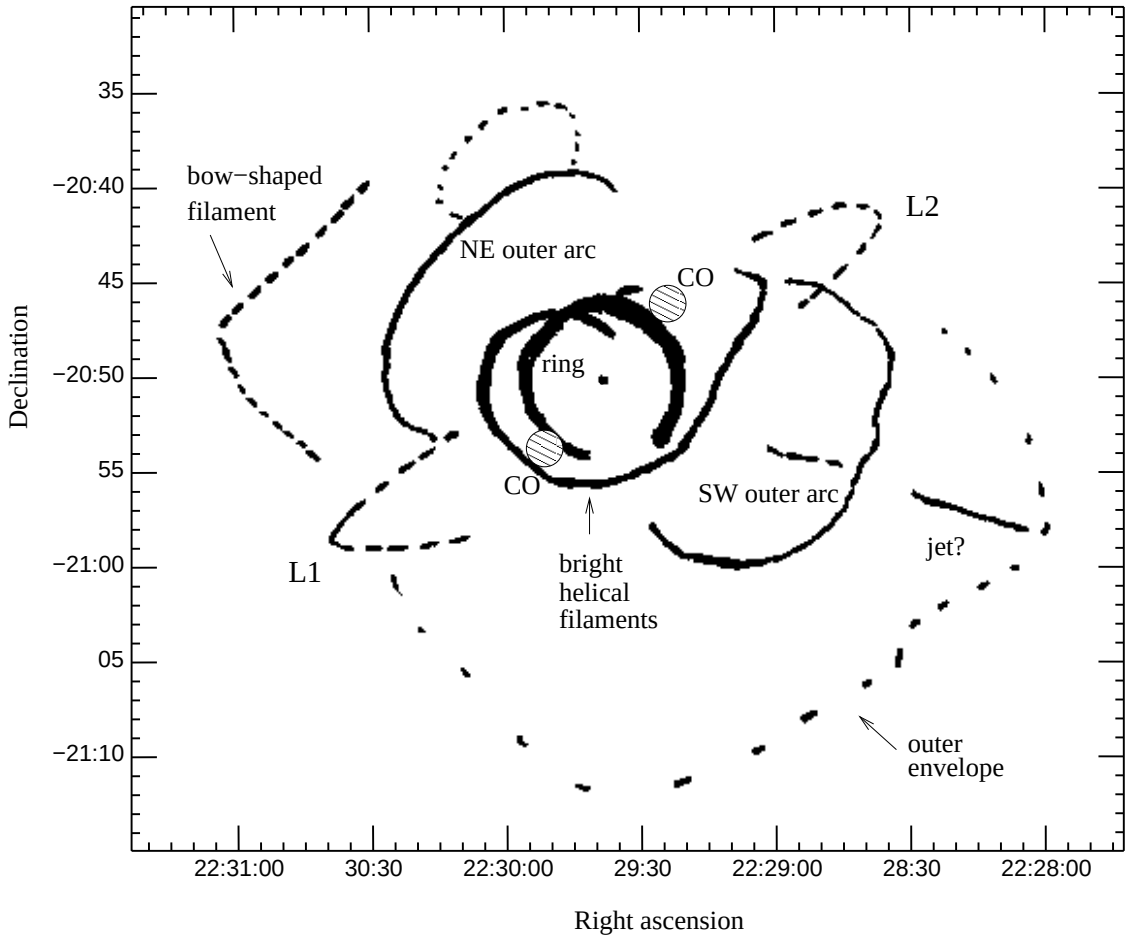

Figure 6. The salient optical and ultra–violet emission features of the large-scale structure of NGC 7293 are compared with the approaching (-50 km s^{-1} – hashed circle to the SE) and receding (+4 km s^{-1} – hashed circle to the NW) parts of the outer CO torus discovered by Young et al (1999). The complete outer torus is not detected in the CO or UV images as it gets confused with the brighter nebular features. The possible bipolar lobes emanating from this outer torus are L1 and L2 in which case they would have receding and approaching radial velocities respectively and would have to have a common axis with it.

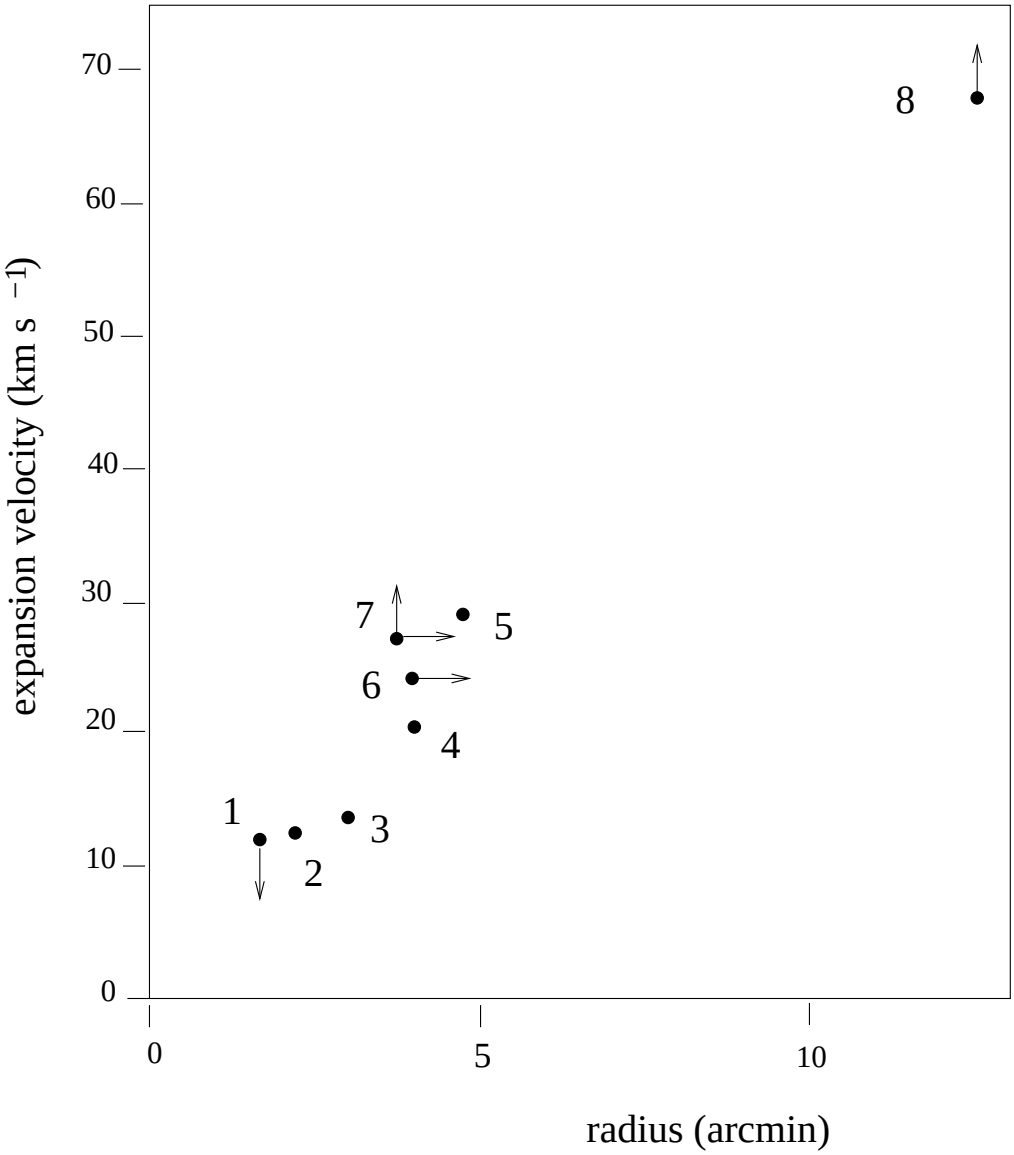

Figure 7. The radial expansions versus radii for the features of NGC 7293 listed as 1 to 8 in Table 1 are shown. Arrowed lines indicate where values are either upper or lower limits for both axes. In the case of 1 i.e. HeII6560Å(Meaburn et al 2005b) the profile is distinctly top-hatted but the separate velocity components not quite resolved. For 7 the tilt to the sight line is unknown affecting both the estimation of the radius and the expansion velocity whereas for 8 the radius is reasonably obtained from the optical image in Fig. 1 but the tilt of the proposed bipolar axis is unknown hence the lower limit for the expansion velocity.